Citation: Journal of Applied Physics 105, 113505 (2009)
https://doi.org/10.1063/1.3123768

Optical constants of evaporation-deposited silicon monoxide films in the 7.1 – 800 eV photon energy range

Mónica Fernández-Perea, Juan I. Larruquert, José A. Aznárez, José A. Méndez, Manuela Vidal-Dasilva

Instituto de Física Aplicada-Consejo Superior de Investigaciones Científicas, C/ Serrano 144, 28006 Madrid, Spain, phone: +34 91 561 8806, fax: +34 91 411 7651,

email: larruquert@ifa.cetef.csic.es

Eric Gullikson, Andy Aquila

Center for X-ray Optics, Lawrence Berkeley National Laboratory, Berkeley, CA 94720, USA

Regina Soufli

Physics and Advanced Technologies, Lawrence Livermore National Laboratory, Livermore, CA 94550, USA

OCIS Codes: 260.7200, 230.4170, 120.4530, 310.6860

The transmittance of silicon monoxide films prepared by means of thermal evaporation was measured from 7.1 to 800 eV and used to determine the optical constants of the material. SiO films deposited onto C-coated microgrids in ultra high vacuum conditions were measured *in situ* from 7.1 to 23.1 eV. Grid-supported SiO films deposited in high vacuum conditions were characterized *ex situ* from 28.5 to 800 eV. At each photon energy, transmittance and thickness data were used to calculate the extinction coefficient, *k*. The combination of the obtained *k* values with data from the literature, interpolations and extrapolations provided a set of *k* values in the whole electromagnetic spectrum, that was used in a Kramers-Kronig analysis to obtain the real part of the

index of refraction, *n*. Two different sum-rule tests were performed, that indicated good consistency of the data.

1. INTRODUCTION

Silicon monoxide films have been widely used as protective layers[1], antireflecting layers[2] and multilayer spacers[3] in coatings for the visible and IR spectral ranges, and also as a replica and support material in the preparation of samples for electron microscopy[4]. In spite of the wide range of optical applications, the optical constants of SiO films have not been determined in most of the extreme ultraviolet (EUV, ~12 to 250 eV) and soft x rays (SXR, ~250 eV to several keV) spectral regions.

From a previous work on the optical properties of SiO[5], it is known that this material is more transparent than SiO_2 in the spectral region from 11 to 25 eV. On the opposite side, it is less transparent than SiO_2 in the near UV and visible intervals. Additionally, its low vapor pressure when compared to Si or SiO_2 makes SiO films deposited onto room temperature substrates more uniform and adherent than their Si or SiO_2 counterparts[6]. Therefore, SiO thin films are expected to be suitable as protective layers for coatings in the spectral interval from 11 to 25 eV due to their relatively low absorption and good mechanical properties. A possible application of SiO protective layers in this interval would be their use as capping layers on lanthanide coatings. Lanthanides have been proposed recently as multilayer components for the EUV[7], and their strong reactivity makes the use of a protective layer mandatory. The optical characterization of SiO films at EUV and SXR photon energies is also interesting from a theoretical point of view.

Philipp[5] obtained the dielectric function of SiO films from ~1.5 to 26 eV by applying the Kramers-Kronig analysis to reflectance measurements performed from 1.5 to 25 eV. The author also obtained the absorption coefficient from transmittance measurements in the interval from 1.5 to 9 eV. These data were taken into account in order to carry out an adequate extrapolation of reflectance at energies larger than 25 eV. We have found that the extinction coefficient data calculated by using the absorption coefficient from Fig. 3 of Ref. 5 and the dielectric function from Fig. 5 of Ref. 5 are in disagreement for energies above ~5 eV. According to Philipp in Ref. 8, caution must be taken for energies above 12 eV because of the dependence of the dielectric function on the extrapolation of reflectance. Ref. 8 recommends to perform new measurements above 25 eV in order to improve the accuracy of the high energy data of Ref. 5. Tarrio and Schnatterly[9] used inelastic electron scattering (IES) spectra to determine the absorption coefficient α of SiO films from 90 to 170 eV, the imaginary part of the dielectric function ε_2 from 2 to 20 eV and the absolute loss function $\mathrm{Im}(-1/\varepsilon)$ from 2 to 40 eV.

Outside the spectral region covered in the present work, Hass and Salzberg[1] determined the extinction coefficient *k* of SiO films in the spectral ranges from 0.089 to 0.155 eV and from 2.25 to 5.17 eV. The real part of the index of refraction *n* was calculated from 0.089 to 5.17 eV. The dependence of the films stoichiometry on the base pressure and deposition rate was also studied. It was found that both slow evaporation in high vacuum (HV, base pressure ~10^{-4} Pa) and heating in air produced a deviation of the SiO stoichiometry so that the O-to-Si-atom ratio was higher than unity. The resulting SiO_x $(x > 1)$ films showed in the whole studied spectral range lower absorption in the UV and lower index of refraction than stoichiometric SiO films. Hjortsberg and Granqvist[10] reported dielectric function values in the spectral range from 0.0368 to 0.155 eV. Their

results are in very good agreement with Ref. 1 in the overlapping region. López and Bernabeu[11] and Pérez et al. [3,12] determined the complex refractive index $N = n + ik$ from transmittance measurements of SiO films deposited at various substrate temperatures in the spectral range from 0.207 to 0.992 eV. Rawlings[13], Hirose and Wada[14] and Cremer et al.[15] reported the extinction/absorption coefficients of SiO films within the intervals 1.46 – 2.76 eV, 2.48 – 3.81 eV and 2.07 – 4.96 eV, respectively. In all the aforementioned references SiO thin films were deposited by thermal evaporation in HV systems.

The goal of the present work is to obtain reliable SiO optical constants from transmittance measurements performed on thin films deposited by evaporation in HV or ultra-high vacuum (UHV) conditions in the EUV and SXR spectral ranges, where most of the data are lacking or need to be revised. Section 2 describes the experimental techniques used in this work. Section 3 reports on the experimental results: the calculation of the extinction coefficient from the slope of transmittance versus thickness data and the Kramers-Kronig analysis that provides the real part of the index of refraction. Inertial and *f* sum rules provided a way to check the quality of both the real and imaginary parts of the obtained index of refraction.

2. EXPERIMENTAL TECHNIQUES

The extinction coefficient values presented below were calculated from transmittance (*T*) measurements performed onto samples with SiO thin films of different thicknesses. *T* is related to SiO thickness (*d*) by the approximate relation

$$Ln(T) \approx A + \left(-\frac{4\pi k}{\lambda} \right) \cdot d \,, \qquad (1)$$

were λ stands for the radiation wavelength and *A* is a constant that accounts for the substrate transmittance and for the reflectance at the vacuum-SiO interface. A common oxide or hydrocarbon layer which may be present on the surface of the samples would also contribute as an additive constant to Eq. (1), and therefore would not interfere with *k* determination. At each photon energy, a straight line was fitted to the experimental *Ln(T)* vs *d* data by the method of least squares. For Eq. (1) to be correct it is necessary that multiple reflections inside the SiO film are negligible. In the present case this condition is fulfilled because at low energies the absorption of the film is high, and at high energies the reflectivity at the film interfaces is low.

Samples were prepared by means of thermal evaporation at the Grupo de Óptica de Láminas Delgadas (GOLD) at Instituto de Física Aplicada, Consejo Superior de Investigaciones Científicas (Spain). The measurements were split into two groups attending to the photon energy. Measurements from 7.1 to 23.1 eV were performed *in situ* in UHV conditions at GOLD. For energies above 28.5 eV the measurements were performed *ex situ* at the 6.3.2 beamline at ALS synchrotron, Berkeley (USA).

2.1 Transmittance measurements from 7.1 to 23.1 eV at GOLD:

The experimental equipment at GOLD consists of a far and extreme ultraviolet (FUV-EUV) reflectometry chamber at UHV pressure attached to an UHV preparation chamber. Ion and Ti sublimation pumping systems provide a base pressure of 1×10^{-8} Pa after baking at 470 K. The chambers are connected in vacuum so that samples are maintained under UHV conditions from deposition to optical characterization. A complete description of the experimental equipment can be found elsewhere[16].

Four SiO thin films with increasing thickness were deposited successively onto the same substrate by means of thermal evaporation from Ta boats, and the transmittance of the films was measured immediately after each deposition. Pressure during evaporation ranged from 2×10^{-7} to 2×10^{-6} Pa, and deposition rate was maintained from 3 to 5 nm/min. We followed the recommendations of Ref. 6 regarding the temperature of the evaporation source, which must be maintained at about 1520 K in order to obtain stoichiometric SiO films. The electrical parameters which provided a source temperature of ~1520 K were calibrated with an optical pyrometer. The distance from the evaporation source to the substrate was 38 cm. SiO raw material was purchased to Cerac Inc., and it had a nominal purity of 99.97%. Thickness was controlled with a quartz crystal monitor that had been previously calibrated by means of Tolansky interferometry[17]. After extracting the samples from the vacuum chamber, the thickness was measured by using the aforementioned interferometric technique on a glass witness located close to the sample during depositions. The individual film thicknesses were 17.3, 27.2, 37.1 and 47.0 nm as determined from the total thickness measured by Tolansky along with the nominal film thicknesses to total thickness ratios.

Substrates consisted of Ni microgrids with a nominal open area of 88.6% on which a ~12 nm-thick C thin film had been deposited. We used microgrids with squared holes of 203 μm per side separated by bars 12.7 μm thick. The thickness of the grids was 15 μm. The high transmittance of these grid-supported thin-film substrates makes possible to perform transmittance measurements at FUV, EUV and SXR wavelengths. C films were deposited by evaporation with an electron gun on the microgrid coated with a collodion film. The collodion was later dissolved in amyl acetate.

Eq. (1) is a good approximation provided that multiple reflections inside the SiO film are negligible. The contribution of multiple reflections to the transmittance depends simultaneously on the reflectance at the SiO inner interfaces, the film absorption and the film thickness. In the case of absorbing materials such as SiO in the studied spectral region, Eq. (1) will be correct for thickness values larger than a threshold.

The procedure to know whether Eq. (1) was applicable in our case consisted in plotting the experimental data of *Ln(T)* versus *d*. We only used those thicknesses which gave linear dependencies between *Ln(T)* and *d*. For photon energies below 11.8 eV the thinnest film (17.3 nm) did not comply with the linearity requisite, so it was not used. At energies above 11.8 eV the signal transmitted by the thicker film was extremely low, and therefore it was not used either. After the calculation of the optical constants the validity of Eq. (1) was further verified by means of the exact calculation of the *Ln(T)* versus *d* plots, including the multiple reflections contribution. This was performed with the usual equations based on Fresnel coefficients. The result is shown in Figure 1 for photon energies of 7.1 and 11 eV. The curves correspond to the transmittance of a self-supported SiO film as a function of thickness calculated from the obtained optical constants (see section 3). From the linearity range of the curves it is concluded that Eq. (1) is correct for the selected film thicknesses. The same is applicable to the rest of the 7.1 to 23.1 eV interval.

The EUV-FUV radiation source at GOLD is a windowless capillary discharge lamp connected to the reflectometer chamber through a differential pumping system that maintains a pressure gradient from about 100 Pa in the lamp exit to 1.5×10^{-7} Pa in the reflectometer during lamp operation. By using a quadrupole mass spectrometer it was

seen that the main component of the residual atmosphere in the reflectometer is the nonoxidizing gas mixture flowing through the discharge lamp. To measure the transmittance of a sample, the beam intensity was measured first directly and then with the sample in the radiation path.

2.2 Transmittance measurements from 28.5 to 800 eV at 6.3.2 beamline:

Samples consisted of SiO thin films of five different thicknesses supported on Ni microgrids similar to those described in the previous section. SiO deposition was performed at GOLD, in a HV system with a turbomolecular pumping and a base pressure of 8×10^{-5} Pa. The samples were prepared by using the same technique that was used to prepare the C substrates as described in section 2.1. SiO films were condensed onto collodion coated microgrids and the collodion was later dissolved in amyl acetate. SiO raw material was purchased to Balzers, and it had a nominal purity of 99.8%. The distance from the evaporation source, a Ta boat, to the substrate, was 30 cm. Evaporation rate was maintained at about 6 nm/min, corresponding to a source temperature of about 1520 K. Thicknesses were controlled with a quartz microbalance and measured after venting the chamber by means of Tolansky interferometry performed on a glass witness. The individual film thicknesses were 19.4, 39.7, 58.4, 118.0 and 160.5 nm.

Regarding the validity of Eq. (1), experimental *Ln(T) vs d* plots showed a good linearity for all the thicknesses and photon energies. Figure 1 shows the exact calculation of the transmittance of a SiO film onto a 12-nm thick C film for photon energies of 28.5 and 100 eV as a function of SiO film thickness. We used SiO optical constants coming from this work and C optical constants from a previous work[18]. From the linearity range of

the curves it is concluded that Eq. (1) is correct for the selected film thicknesses. The same is applicable to the rest of the 28.5 to 800 eV interval. Transmittance measurements were performed after ~1 month of exposure to the atmosphere.

We also determined the SiO films density by weighing a piece of Al foil of known area before and after it was coated with a SiO film of known thickness. The resulting density value was 2.17 ± 0.05 g/cm^3, which is consistent both with the density value of bulk SiO (2.15 g/cm^3) and of thin film SiO (2.18 g/cm^3) from the literature[6].

The characteristics of the 6.3.2 beamline at ALS and its measurement chamber have been described in detail earlier[19,20]. A variable-space grating monochromator utilizing 80-, 200-, 600-, and 1200-line/mm gratings was used to access the photon energy from 28.5 to 800 eV. The monochromator exit slit was set to a width of 50 μm for all transmittance measurements. Depending on the photon energy and grating used, the spectral resolving power varied from 300 to 3500 across the 28.5–800-eV region. Energy was calibrated based on absorption edges of filters installed at the beamline, with a relative accuracy of 0.04% to 0.011% rms (depending on photon energy) and with 0.007% to 0.05% repeatability. Second-harmonic and stray-light suppression at various energies were achieved with a selection of filters installed at the beamline. At low energies, where higher harmonics are present, an order suppressor consisting of three grazing-incidence mirrors was used in addition to filters. Any residual broadband scattered light from the beamline is suppressed with use of trimming slits located just upstream of the reflectometer. In this way, a spectral purity of 99.9% or better is achieved throughout the beamline spectral range. The ALS storage ring current was used to normalize the signal against the storage ring current decay. The base pressure in

the measurement chamber was 10^{-4} Pa. The signal was collected on a Si photodiode detector with a 10x10-mm^2 active area and acceptance angle of 2.4°. In this case the size of the beam spot (50 × 300 μm FWHM) and the grid holes were comparable, and a precise positioning of the sample was necessary in order to obtain a maximum signal both for the direct and transmitted beams.

3. RESULTS AND DISCUSSION

3.1 Transmittance and extinction coefficient data

Transmittance of the SiO films deposited onto the thin C film substrate from 7.1 to 23.1 eV are shown in Figure 2. The highest absorption observed at about 16 eV is due to a combination of SiO absorption and the maximum absorption of C at about 15 eV. Transmittance of grid-supported SiO films from 28.5 to 800 eV is displayed in Figure 3. There are dips in transmittance associated with the Si $L_{2,3}$ absorption edge[21] at 99.8 and 99.4 eV and the O K absorption edge at 543.1 eV. The C K absorption edge at 284.2 eV indicates the presence of carbon in the surface of the samples. The transmittance plotted in Figs. 2 and 3 is reduced by a constant factor due to the presence of the microgrid.

The extinction coefficient data was calculated from the slope of *Ln(T)* versus thickness using Eq. (1). This method neutralizes out the contribution of the microgrid, of the substrate present in Fig. 2 and of any common oxide or hydrocarbon layers which may be present in the surface of the SiO films. Figure 4 shows the calculated extinction coefficient data in the covered spectral range. The complete absence of the C K edge at 284.2 eV suggests that any carbon contamination must be common to all the samples characterized ex situ. Figure 4 displays also data from the literature. At low energies we have plotted the two sets of extinction coefficient values from Philipp (calculated from

data of Figs. 3 and 5 of Ref. 5). As mentioned before, the two sets are very similar for photon energies up to ~5 eV, but at higher energies we observe considerable differences. Data from this work are in very good agreement with *k* values from Fig. 3 of Ref. 5 in the overlapping region. At photon energies larger than 30 eV the data plotted on Fig. 4 of this work was downloaded from the CXRO web page[22] for SiO with a density $\rho_{SiO} = 2.17 \pm 0.05$ g/cm^3.

Ref. 22 calculates the refractive index $\mathcal{N}$ of a compound from the atomic scattering factors of the constituent elements (f_j) in the independent atom approximation,

$$\mathcal{N} = n + ik = 1 - \delta + ik = 1 - \frac{1}{2\pi} r_0 \lambda^2 \sum_j N_j^{at} f_j \,, \qquad (2)$$

where $\delta = 1 - n$, r_0 is the classical electron radius, λ is the wavelength of the radiation and N_j^{at} are the atomic densities of the constituent elements. From the experimental density it is possible to obtain N_{Si}^{at} and N_O^{at} from

$$N_{Si}^{at} = N_O^{at} = \rho_{SiO} / m_u \left(A_{Si} + A_O \right), \qquad (3)$$

where m_u is the atomic mass unit and A_{Si}, A_O are the atomic weights of Si and O, respectively. In the case of Si the atomic scattering factors come from experimental optical constants[23] for energies in the 30 to 500 eV interval, and from Henke et al.[24] in the rest of the spectrum. In the case of O the atomic scattering factors come entirely from Ref. 24. The independent atom approximation is valid for photon energies larger than about 30 eV and sufficiently far from absorption edges. Fig. 4 shows a good agreement between *k* data from this work and *k* data from CXRO except for photon energies close to the absorption edges.

The uncertainty of the extinction coefficient was estimated in the following way: a computer code was used to simulate additional measurements by adding random errors to the experimental measurements; at every simulated measurement, transmittance and thickness values were randomly modified within the limits imposed by their relative uncertainties (estimated in ~0.02 in the case of transmittance and ~0.05 in the case of thickness). With these modified values, the extinction coefficient was calculated in the usual way through the slope of *Ln(T)* versus thickness. After a large number of measurement simulations, the standard deviation σ_k of the resulting set of extinction coefficient values was interpreted as δk, the uncertainty of k, with k taking values within $k \pm \delta k$. As a result of this procedure the relative uncertainty $\delta k/k$ of the SiO extinction coefficient was determined to be between ~±1% and ±4% in the whole studied spectral range.

Figures 5 and 6 show in more detail the extinction coefficient near the Si $L_{2,3}$ and O K absorption edges, along with values from the literature. k values at both edges differ substantially from CXRO data because the independent atom approximation is not valid at the absorption edges. When compared to Tarrio and Schnatterly[9] data near the Si $L_{2,3}$ edge, k values are substantially different, and the peaks are broader and located at similar photon energy values.

3.2 Refractive index calculation with the dispersion relations

In order to obtain a complete set of extinction coefficient values in the entire electromagnetic spectrum we gathered data from the literature in the following way: Hjortsberg and Granqvist[10] extinction coefficient values were used from 0.0368 to 0.089 eV. These data connected smoothly with k values from Hass and Salzberg[1], which were

used up to 0.155 eV. From Perez and Sanz[12] we obtained *k* values in the interval 0.42 – 0.992 eV. Considering that extinction coefficient values from Philipp´s[5] Fig. 3 are in good agreement with ours in the overlapping region, we used these values in the interval 1.5 – 7.1 eV instead of data coming from Philipp´s[5] Fig. 5. *k* data downloaded from the CXRO web page[22], which were calculated with the experimentally determined density, were used from 800 eV up to 3×10^4 eV. The gaps from 0.155 to 0.42 eV, 0.992 to 1.5 eV and 23.1 to 28.5 eV were filled by using smooth interpolations. An extrapolation to zero energy was performed by fitting the low energy data from Ref. 10 to the function $k = k_0 (E/E_0)^{\beta}$, with $\beta = 1.348$. k_0 = 0.579 is the extinction coefficient value at a photon energy E_0 = 0.0368 eV, which is the smallest photon energy where there are available *k* values in the literature. Another extrapolation was performed at energies higher than 3×10^4 eV in which we maintained constant the slope of data from Ref. 22. This assumption resulted in a function of the form $k = k_0 (E/E_0)^{\beta}$ with $\beta = -3.880$, $k_0 = 6.699\times10^{-10}$ and $E_0 = 3\times10^4$ eV, the highest photon energy were there are available values in the literature. The obtained complete set of extinction coefficient data is displayed in Figure 7.

The consistency of the *k* data set has been evaluated by means of the *f*-sum rule[25], which may be written in the following form:

$$n_{eff}(E) = \frac{4\varepsilon_0 m}{\pi N_{SiO} e^2 h^2} \int_0^E E' k(E') dE' . \qquad (4)$$

This equation provides the number of electrons per molecule contributing to SiO absorption up to a photon energy *E*. ε_0 stands for the permittivity of vacuum, *m* is the electron mass, *h* is Planck's constant and N_{SiO} is the number of SiO molecules per unit

volume. The limit of n_{eff} at high energies must converge to the total number of electrons of the SiO molecule, which is $Z_{SiO} = Z_{Si} + Z_O = 22$. The limit calculated with Eq. (4) is 21.43, which is only 2.6% lower than the expected value. We conclude that the *f*-sum rule test, evaluated with the complete set of *k* values, results in a satisfactory value.

The complete set of extinction coefficient data was used to calculate the real part of the index of refraction of SiO films by means of the Kramers-Kronig relation:

$$n(E) - 1 = \frac{2}{\pi} P \int_0^\infty \frac{E' k(E')}{E'^2 - E^2} dE', \tag{5}$$

where *P* stands for the Cauchy principal value. Note that in order to obtain *n* at a single photon energy it is necessary to know the extinction coefficient of the material in the whole electromagnetic spectrum.

Figure 8 displays the calculated *n* values from 5 to 50 eV, along with data from the literature. At energies lower than ~8 eV present data match well Philipp's data, which were calculated from the dielectric function displayed in Fig. 5 of Ref. 5. On the other hand, there are differences above ~8 eV. This result is in agreement with Philipp's warning of Ref. 8 about data of Ref. 5. Tarrio and Schnatterly[9] data do not match either current data or Philipp's. At higher energies, CXRO data are very similar to present data.

Figure 9 shows the calculated δ values from about 14 to 800 eV along with CXRO data. A good coincidence is observed except for photon energies close to the absorption edges, which are plotted in detail in Figures 10 and 11.

The evaluation of the consistency of *n* data was performed by means of the inertial sum rule,

$$\int_0^\infty [n(E)-1]dE = 0, \tag{6}$$

which expresses that the average of the refractive index throughout the spectrum is unity. The following parameter is defined to evaluate how close to zero the integral of Eq. (6)[25] is:

$$\zeta = \frac{\int_0^\infty [n(E)-1]dE}{\int_0^\infty |n(E)-1|dE}. \tag{7}$$

Shiles et al.[25] suggested that a good value of ζ should stand within ±0.005. We obtained an evaluation parameter of −0.0008, well below the aforementioned limit, which supports the consistency of the obtained real part of the index of refraction.

4. CONCLUSIONS

Optical constants of evaporated SiO films have been obtained from transmittance measurements in the spectral range from 7.1 to 800 eV, where most of the data either was lacking or needed to be revised. The extinction coefficient (*k*) was calculated directly from transmittance measurements. The Kramers-Kronig analysis provided a way to calculate the real part of the index of refraction (*n*). The extinction coefficient was firstly obtained from transmittance measurements for energies above 10 eV. We believe our data to be more consistent than previous experimental data available in the literature[5] in the spectral range from 10 to 25 eV. As far as we know the real part of the index of refraction was experimentally determined for the first time at energies higher than 28.5 eV. We checked the consistency of the optical constants with both *f*- and

inertial- sum rules. The low absorption of SiO films compared to other stable materials, along with its capability of forming thin uniform layers make this material very promising as a protection layer for lanthanide multilayers working at the EUV.

ACKNOWLEDGMENTS

This work was supported by the National Programme for Space Research, Subdirección General de Proyectos de Investigación, Ministerio de Ciencia y Tecnología, project numbers ESP2002-01391 and ESP2005-02650. This work was also performed under the auspices of the U.S. Department of Energy by the University of California Lawrence Berkeley National Laboratory under contract No. DE-AC03-76F00098, and by the University of California Lawrence Livermore National Laboratory under Contract No. W-7405-ENG-48. M. Fernández-Perea is thankful to Consejo Superior de Investigaciones Científicas (Spain) for funding under the Programa I3P (Ref. I3P-BPD2004), partially supported by the European Social Fund. M. Vidal-Dasilva acknowledges financial support from a FPI BES-2006-14047 fellowship. We acknowledge the technical assistance of José M. Sánchez-Orejuela.

Figure captions

Fig. 1. Calculated natural logarithm of the transmittance of SiO samples as a function of SiO film thickness for several photon energies.

Fig. 2. The transmittance of SiO films deposited onto a grid-supported C thin film substrate as a function of photon energy from 7.1 to 23.1 eV. Measurements were performed *in situ* at GOLD, CSIC. The thickness of each film is indicated.

Fig. 3. The transmittance of grid-supported SiO films as a function of photon energy (log scale) from 28.5 to 800 eV. Measurements were performed *ex situ* at beamline 6.3.2, ALS synchrotron. The thickness of each film is indicated.

Fig. 4. Log-log plot of the extinction coefficient of SiO films versus photon energy. Experimental values from Philipp (taken from Figs. 3 and 5 of Ref. 5) are also displayed. CXRO data, which were calculated for a density value of $\rho_{SiO} = 2.17 \ \ g \cdot cm^{-3}$, are also plotted in the figure.

Fig. 5. Plot of the extinction coefficient of SiO films versus photon energy in the spectral region close to the Si $L_{2,3}$ absorption edge. Experimental values from Tarrio and Schnatterly[9] are also displayed. CXRO data ($\rho_{SiO} = 2.17 \ \ g \cdot cm^{-3}$) are also plotted in the figure.

Fig. 6. Plot of the extinction coefficient (log scale) of SiO films versus photon energy in the spectral region close to the O K absorption edge. CXRO data ($\rho_{SiO} = 2.17 \ \ g \cdot cm^{-3}$) are also plotted in the figure.

Fig. 7. Log-log plot of the extinction coefficient data set versus photon energy used for the Kramers-Kronig analysis. Data from Hjortsberg and Granqvist[10], Hass and Salzberg[1], Perez and Sanz[12] and Fig. 3 of Philipp[5] were used along with the data from this work. CXRO data ($\rho_{SiO} = 2.17 \ \ g \cdot cm^{-3}$) were used from 8×10^2 to 3×10^4 eV.

Fig. 8. Real part of the index of refraction versus photon energy in the low-energy part of the studied spectral range. Experimental values from Tarrio and Schnatterly[9] and Phillip[5] are also displayed. CXRO data ($\rho_{SiO} = 2.17\ \ g{\cdot}cm^{-3}$) are also plotted in the figure for energies larger than 30 eV.

Fig. 9. Log-log plot of $\delta = 1 - n$ versus photon energy in the high-energy part of the studied range. CXRO data ($\rho_{SiO} = 2.17\ \ g{\cdot}cm^{-3}$) are also plotted in the figure for energies larger than 30 eV.

Fig. 10. Plot of δ of SiO films versus photon energy in the spectral region close to the Si $L_{2,3}$ absorption edge. CXRO data ($\rho_{SiO} = 2.17\ \ g{\cdot}cm^{-3}$) are also plotted in the figure.

Fig. 11. Plot of δ of SiO films versus photon energy in the spectral region close to the O K absorption edge. CXRO data ($\rho_{SiO} = 2.17\ \ g{\cdot}cm^{-3}$) are also plotted in the figure.

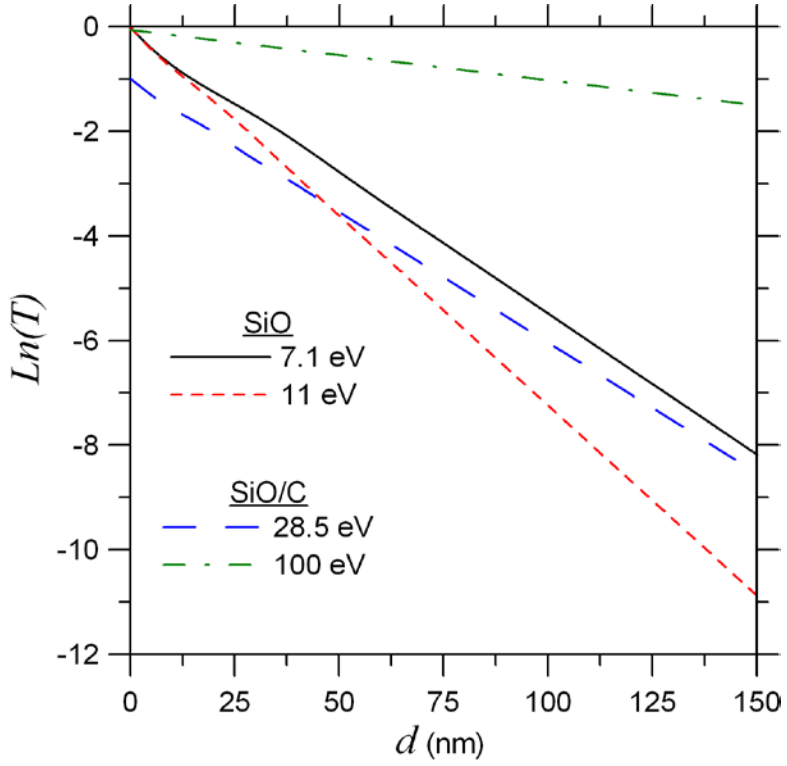
0
-2
-4
-6
-8
-10
-12
Ln(T)
0
25
50
75
100
125
150
d (nm)
SiO
7.1 eV
11 eV
SiO/C
28.5 eV
100 eV

Fig. 1

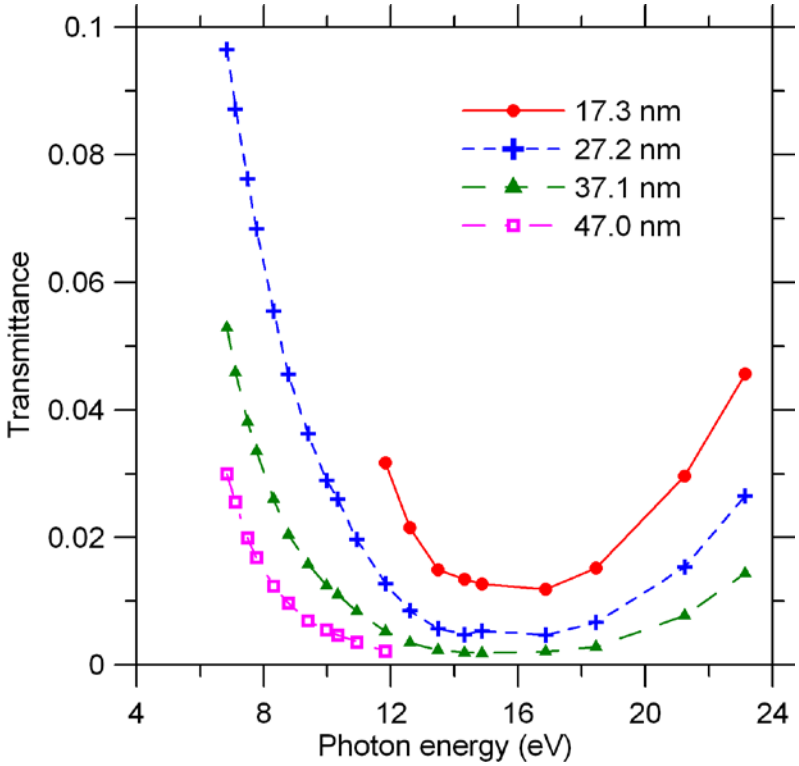
0.1
0.08
0.06
0.04
0.02
0
Transmittance
4
8
12
16
20
24
Photon energy (eV)
17.3 nm
27.2 nm
37.1 nm
47.0 nm

Fig. 2

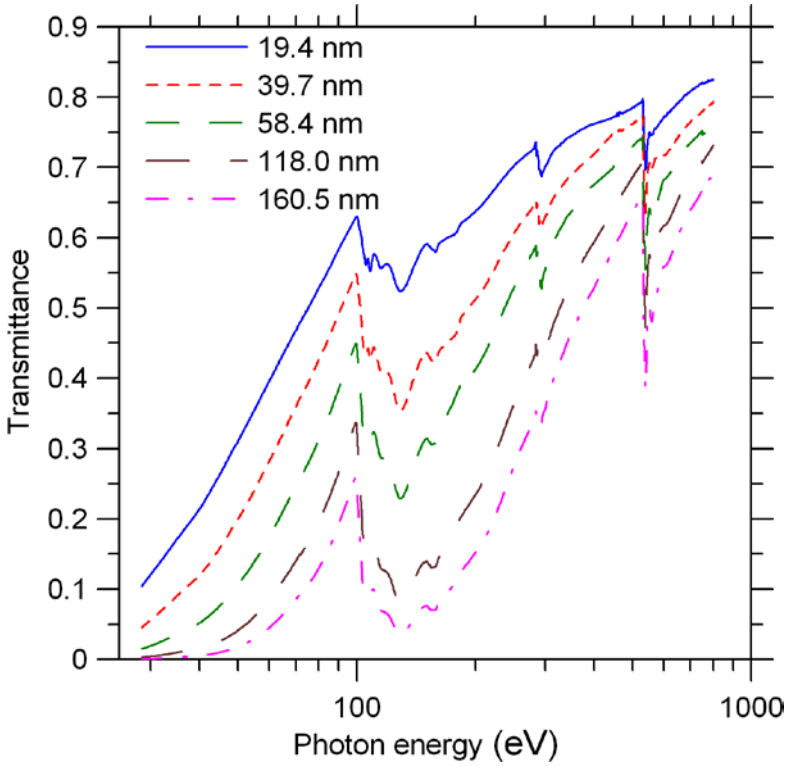
19.4 nm
39.7 nm
58.4 nm
118.0 nm
160.5 nm
Transmittance
0.9
0.8
0.7
0.6
0.5
0.4
0.3
0.2
0.1
0
100
1000
Photon energy (eV)

Fig. 3

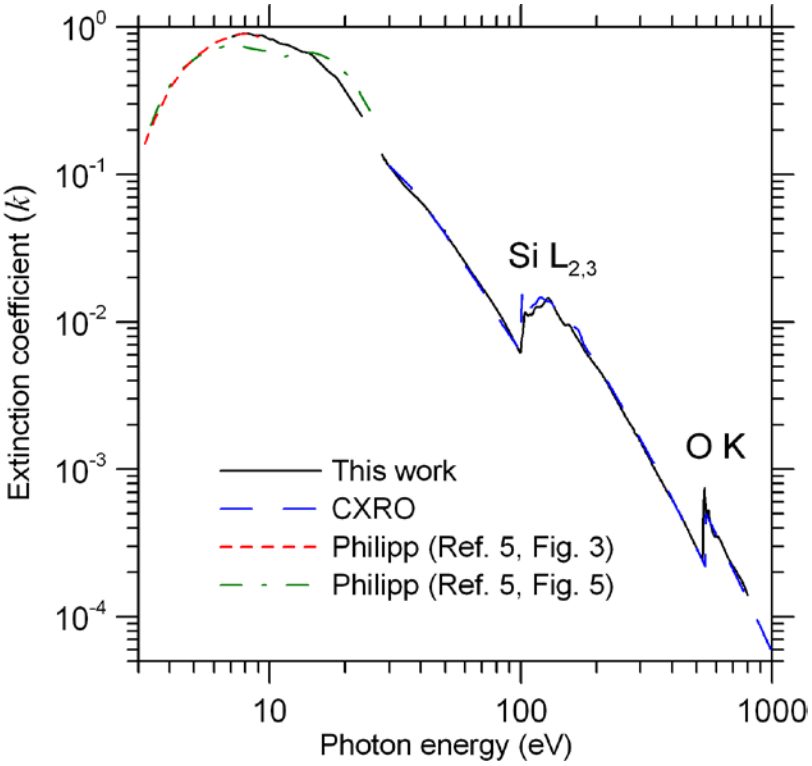
Extinction coefficient (k)
Photon energy (eV)
Si L2,3
O K
This work
CXRO
Philipp (Ref. 5, Fig. 3)
Philipp (Ref. 5, Fig. 5)

Fig. 4

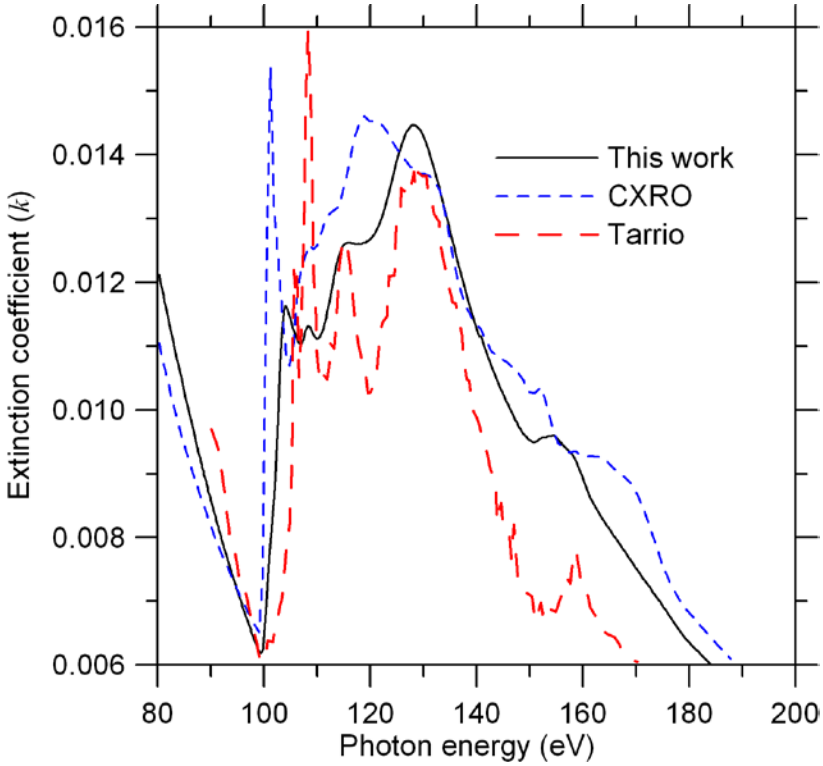
0.016
0.014
0.012
0.010
0.008
0.006
Extinction coefficient (k)
80
100
120
140
160
180
200
Photon energy (eV)
This work
CXRO
Tarrio

Fig. 5

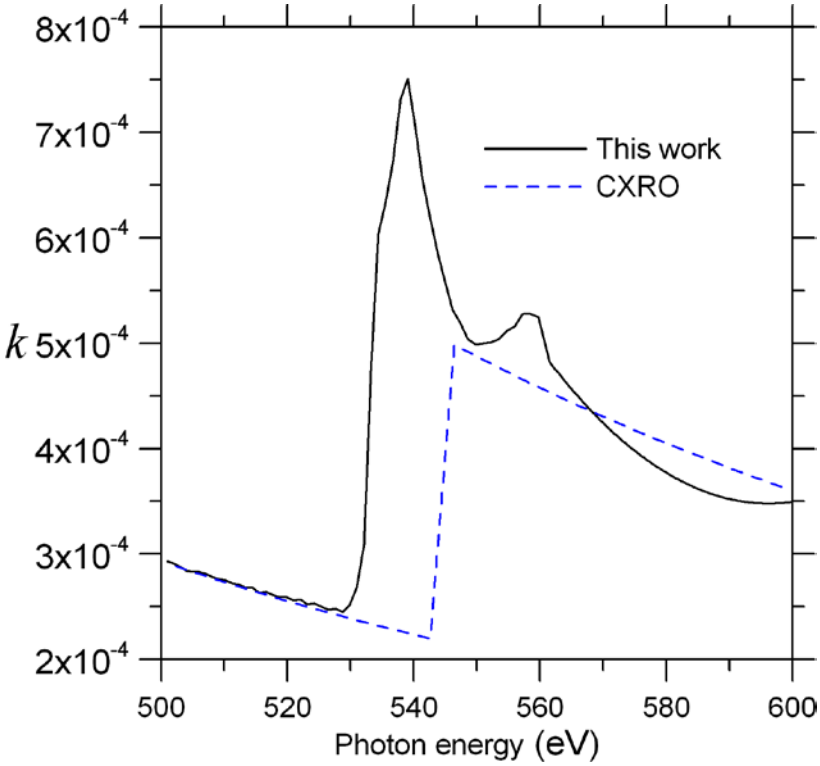
8x10-4
7x10-4
6x10-4
k 5x10-4
4x10-4
3x10-4
2x10-4
500
520
540
560
580
600
Photon energy (eV)
This work
CXRO

Fig. 6

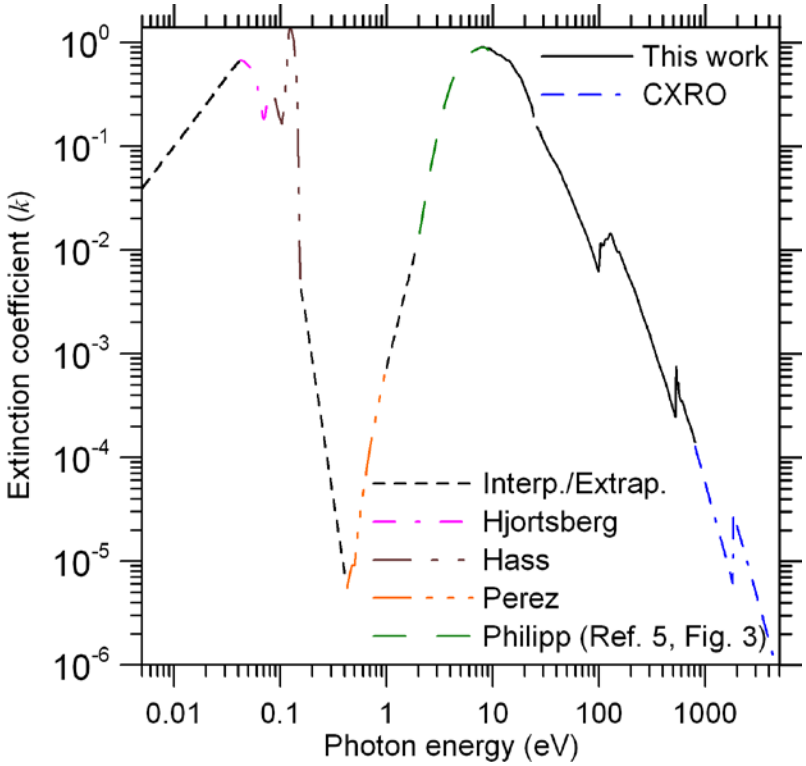
Extinction coefficient (k)
Photon energy (eV)
This work
CXRO
Interp./Extrap.
Hjortsberg
Hass
Perez
Philipp (Ref. 5, Fig. 3)

Fig. 7

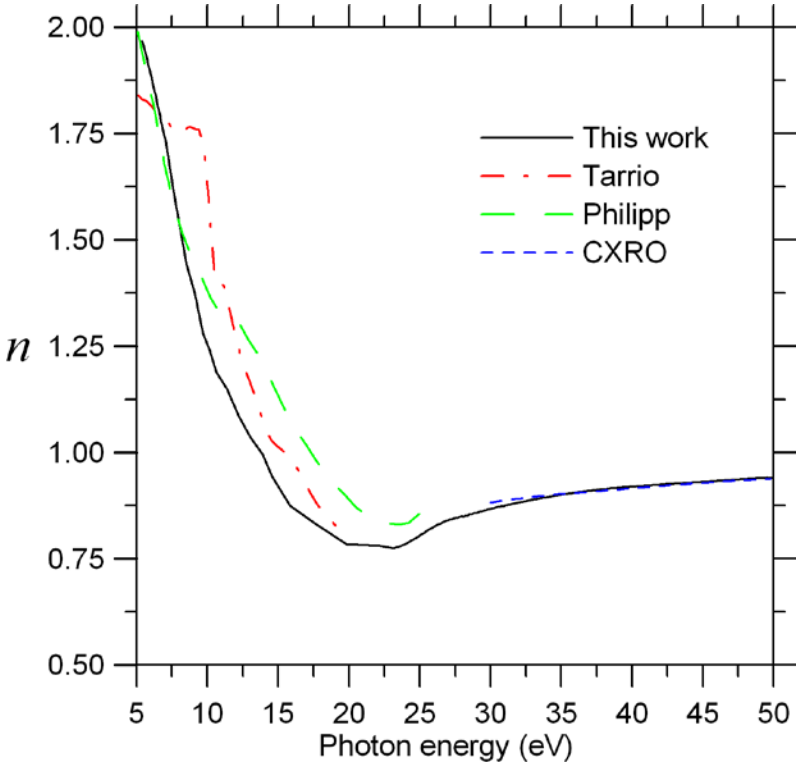
2.00
1.75
1.50
1.25
1.00
0.75
0.50
n
5
10
15
20
25
30
35
40
45
50
Photon energy (eV)
This work
Tarrio
Philipp
CXRO

Fig. 8

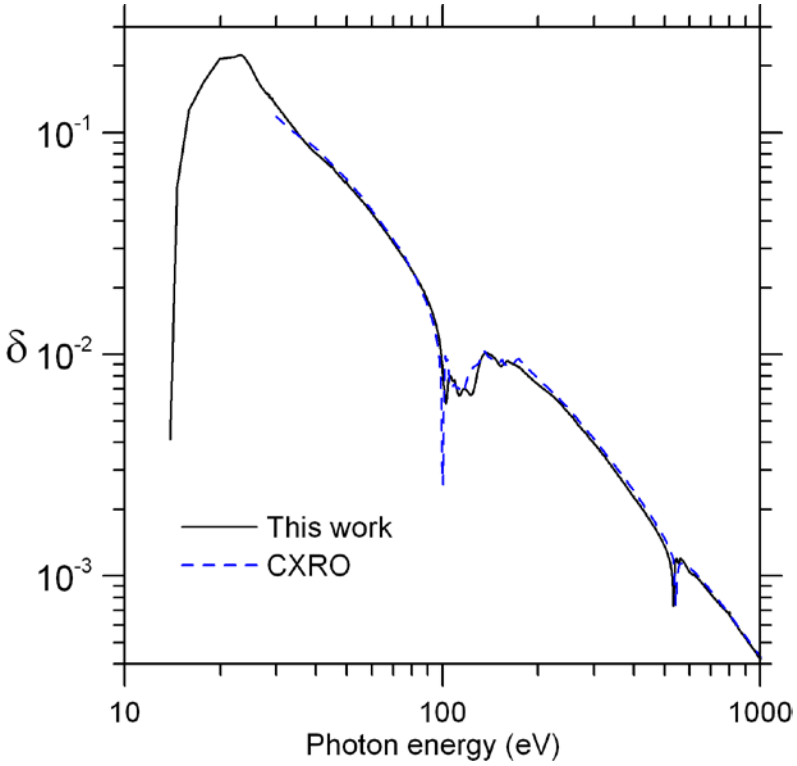

Fig. 9

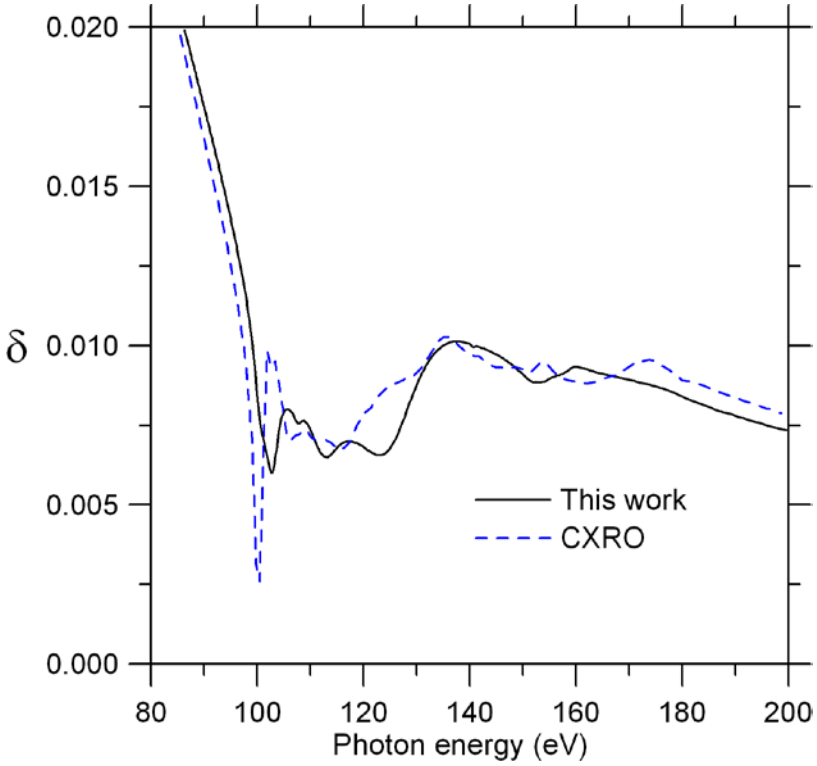
0.020
0.015
0.010
0.005
0.000
δ
80
100
120
140
160
180
200
Photon energy (eV)
This work
CXRO

Fig. 10

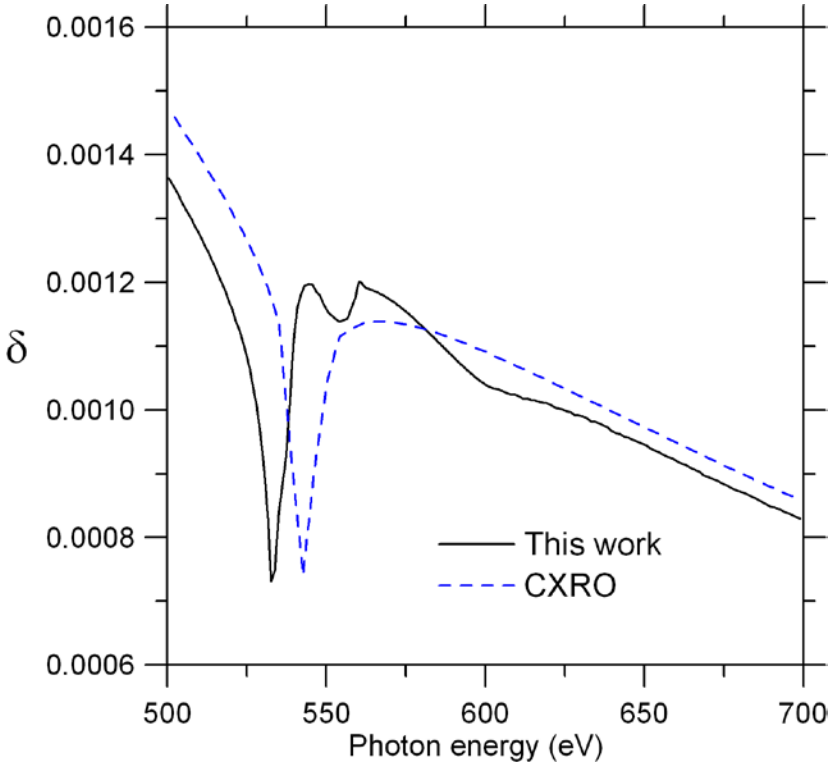
0.0016
0.0014
0.0012
0.0010
0.0008
0.0006
δ
500
550
600
650
700
Photon energy (eV)
This work
CXRO

Fig. 11

References

[1] G. Hass, C. D. Salzberg, “Optical properties of silicon monoxide in the wavelength region from 0.24 to 14.0 microns”, J. Opt. Soc. Am. 44, 181-187 (1954).

[2] G. Hass, H. H. Schroeder, A.F. Turner, “Mirror coatings for low visible and high infrared reflectance”, J. Opt. Soc. Am. 46, 31 (1956).

[3] G. Pérez, A. M. Bernal-Oliva, E. Márquez, J. M. Gónzalez-Leal, C. Morant, I. Génova, J. F. Trigo, J. M. Sanz, “Optical and structural characterization of single and multilayer germanium/silicon monoxide systems”, Thin Solid Films 485, 274-283 (2005).

[4] D.E. Bradley, "The preparation of specimen support films", Chapter 3 in *Techniques for Electron Microscopy*, Desmond Kay, Ed., Blackwell Scientific Publications, Oxford (1961).

[5] H. R. Philipp, “Optical properties of non-crystalline Si, SiO, SiO_x and SiO_2”, J. Phys. Chem. Solids 32, 1935-1945 (1971).

[6] G. Hass, “Preparation, structure, and applications of thin films of silicon monoxide and titanium dioxide”, J. Am. Ceram. Soc. **33**, 353-360 (1950).

[7] M. Fernández-Perea, M. Vidal-Dasilva, , J. A. Aznárez, J. I. Larruquert, J. A. Méndez, L. Poletto, D. Garoli, A. M. Malvezzi, A. Giglia, S. Nannarone, “Determination of the transmittance and extinction coefficient of Pr films in the 4-1,600-eV range”, J. Appl. Phys. 103, 113515-1 to -7 (2008), and references therein.

[8] H. R. Philipp, “Silicon Monoxide (SiO) (Noncrystalline)”, E. D. Palik Ed., *Handbook of Optical Constants of Solids*, 765-769, Academic Press (1985).

[9] C. Tarrio, S. E. Schnatterly, “Optical properties of silicon and its oxides”, J. Opt. Soc. Am. B 10, 952-957 (1993).

[10] A. Hjortsberg, C. G. Granqvist, “Infrared optical properties of silicon monoxide films”, Appl. Opt. 19, 1694-1696 (1980).

[11] F. López, E. Bernabéu, “Refractive index of vacuum-evaporated SiO thin films: Dependence on substrate temperature”, Thin Solid Films 191, 13-19 (1990).

[12] G. Pérez, J. M. Sanz, “Infrared characterization of evaporated SiO thin films”, Thin Solid Films 416, 24-30 (2002).

[13] I. R. Rawlings, “Optical absorption in silicon monoxide”, Brit. J. Appl. Phys. 1, 733-739 (1968).

[14] H. Hirose, Y. Wada, “Dielectric properties and DC conductivity of vacuum-deposited SiO films”, Jpn. J. Appl. Phys. 3, 179-190 (1964).

[15] E. Cremer, Th. Graus, E. Ritter, “Über das absorptionsvermögen dünner siliciumoxydschichten in abhängigkeit vom oxydationsgrad”, Z. Elektrochem. 62, 939-1038 (1958).

[16] J. A. Aznárez, J. I. Larruquert, and J. A. Méndez, “Far-ultraviolet absolute reflectometer for optical constant determination of ultrahigh vacuum prepared thin films”, Rev. Sci. Instrum. 67, 497-502 (1996).

[17] S. Tolansky, *Multiple-Beam Interferometry of Surfaces and Films*, Oxford U. Press, London (1948).

[18] M. Fernández-Perea, J. A. Aznárez, J. I. Larruquert, J. A. Méndez, L. Poletto, D. Garoli, A. M. Malvezzi, A. Giglia, S. Nannarone, “Transmittance and optical constants of Ce films in the 6 – 1200 eV spectral range”, J. Appl. Phys. 103, 073501-1 to -7 (2008).

[19] J. H. Underwood, E. M. Gullikson, “High-resolution, high-flux, user friendly VLS beamline at the ALS for the 50-1300 eV energy region,” J.Electr. Spectr. Rel. Phenom. 92, 265-272 (1998).

[20] E. M. Gullikson, S. Mrowka, B. B. Kaufmann, "Recent developments in EUV reflectometry at the Advanced Light Source," in *Emerging Lithographic Technologies V*, E. A. Dobisz eds., Proc. SPIE 4343, 363-373 (2001).

[21] Electron binding energies were taken from M. Cardona and L. Ley, Eds., *Photoemission in Solids I: General Principles*, Springer-Verlag, Berlin (1978), compiled by G. P. Williams, *X-Ray Data Booklet*, A. C. Thompson and D. Vaughan, Eds., Lawrence Berkeley Laboratory, Berkeley (1986).

[22] E. M. Gullikson, "X-ray interactions with matter", currently available on the World Wide Web http://www-cxro.lbl.gov/optical_constants.

[23] R. Soufli, E. M. Gullikson, "Reflectance measurements on clean surfaces for the determination of optical constants of materials in the EUV/soft x-ray region", Appl. Opt. 36, 5499-5507 (1997).

[24] B.L. Henke, E.M. Gullikson, J.C. Davis, "X-ray interactions: photoabsorption, scattering, transmission, and reflection at E=50-30000 eV, Z=1-92", Atomic Data and Nuclear Data Tables 54, 181-342 (1993).

[25] E. Shiles, T. Sasaki, M. Inokuti, D. Y. Smith, "Self-consistency and sum-rule tests in the Kramers-Kronig analysis of optical data: applications to aluminium", Phys. Rev. B 22, 1612-1628 (1980).